14th International Symposium on Turbulence and Shear Flow Phenomena (TSFP14)
Heidelberg, Germany, July 28–31, 2026

IS THERE A NEW LOG-LAW IN STRATIFIED CHANNEL FLOWS?

Vincent J. Peterhans
Meteorological Institute
University of Hamburg
Bundesstr. 55, 20146 Hamburg, Germany

International Max Planck Research School on Earth System Modeling
Max Planck Institute for Meteorology
Bundesstr. 53, Hamburg 20146, Germany

vincent.peterhans@uni-hamburg.de

Victor Avsarkisov
Meteorological Institute
Bundesstr. 55, University of Hamburg
20146 Hamburg, Germany

Juan Pedro Mellado
Meteorological Institute
Bundesstr. 55, University of Hamburg
20146 Hamburg, Germany

Sergio Hoyas
Instituto Universitario de Matemática Pura y Aplicada
Universitat Politècnica de València
Camino de Vera, 46022 Valencia, Spain

ABSTRACT

The Monin-Obukhov similarity theory emerges as a powerful model for predicting the effects of stratification on the mean velocity profile in a turbulent boundary layer. While its results for the overlap layer are generally very accurate, the theory loses its applicability under strong stratification and towards the edge of the overlap layer. To address these limitations, a modified derivation is presented that focuses on strong stratification and the early overlap region. The approach yields a model that serves as an extension to the classical log-law that takes the effects of stratification into account and is evaluated on a set of direct numerical simulations of a plane Couette flow with varying degrees of stratification. The analysis suggests that a log-law can remain valid for stratified flows when an effective, modified Kármán constant, which considers the effects of strong stratification, is introduced.

INTRODUCTION

One fundamental result of wall-bounded turbulence research is the near-wall logarithmic scaling law for the mean streamwise velocity (Von Kármán, 1931; Tennekes & Lumley, 1972). It has been found to accurately predict the behavior between the buffer layer and core flow for a large variety of high Reynolds-number flows and is characterized by the empirical Kármán constant. While the constant is often used with a unique value of $\kappa = 0.41$ (Schlichting & Gersten, 2016), different works have reported values ranging from 0.38 to 0.43 for various flow conditions and measuring methods (Zagarola & Smits, 1998; Mckeon *et al.*, 2004; Hoyas & Jiménez, 2006*b*; Hoyas *et al.*, 2022). This has raised the question whether the Kármán constant is indeed a constant independent of all other flow quantities. Subsequently, works such as Jiménez & Moser (2007) have shown that an extension to the classical derivations can result in an effective modification of the presumed constant and Monkewitz & Nagib (2023) question its universality based on both numerical simulations and experimental data.

Because the classical log-law does not take the effects of stratification into account, a first modification was proposed by Monin and Obukhov in 1954 using self-similarity theory to extend its applicability (Monin & Obukhov, 1954). In many works, such as the analysis of atmospheric measurements by Businger *et al.* (1971), the model has since proven to be a powerful predictor for mean velocity profiles. Subsequently, various aspects of turbulent, stratified flows have been studied, among them intermittency (Ansorge & Mellado, 2016; Deusebio *et al.*, 2015), effects on the emergence of large-scale structures (Gandía-Barberá *et al.*, 2021) and specific application cases such as the convective atmospheric boundary layer that drives surface-atmosphere interactions (Fodor *et al.*, 2019; Tong & Ding, 2020). One notable result of these more recent works is the failure of Monin-Obukhov self-similarity theory (MOST) under conditions of intermittency, unstable stratification, and strong stable stratification, with a large amount of empirical evidence from measurements in the atmospheric boundary layer (Stiperski & Calaf, 2023; Mahrt, 1998; Grachev *et al.*, 2005; Foken, 2006). Moreover, as recognized by Monin & Obukhov (1954), the classical model is by construction only valid in the so-called overlap region, while becoming increasingly inaccurate for smaller wall-distances. These shortcomings can have a direct impact on predictive models that use their assumptions or rely on measurements from outside the validity region, resulting in, for example, overestimated surface cooling in atmospheric models under certain conditions (Mahrt, 1998). Correspondingly, a wide variety of solutions and improvements to the theory have been proposed, ranging from different definitions of the driving length-scales (Mater & Venayagamoorthy, 2014; Yano & Waclawczyk, 2022) to the proposition of incomplete self-similarity by including explicit dependencies on Reynolds and Prandtl number (Barenblatt & Monin, 1979) or the evaluation of alternate power-law-based approaches (Barenblatt & Chorin, 1997). Recent works by Cheng *et al.* (2023) have moreover shown that a logarithmic law may still exist in stratified conditions as an alternative to MOST, which can be uncovered by considering a modification of the classically unique Kármán constant to include a dependency on stratification.

This work aims to provide a theoretical foundation and additional empirical evidence for a stratified log-law as reported by Cheng *et al.* (2023). A reasoning similar to Jiménez & Moser (2007) is used to derive an effective modification of the Kármán constant by combining their approach with classical MOST and the additional consideration of strong stratification. The result are two model equations for mean streamwise velocity and temperature, which resemble a stratified log-law and successfully match the observations of Cheng *et al.* (2023). Following the derivation, a set of high-resolution DNS data of a plane Couette flow with varying degrees of stratification is used to validate and contextualize the found equations in relation to underlying physical phenomena, while last conclusions are given in the final section.

DERIVATION OF A MODIFIED LOG-LAW

The analytical model for the mean velocity profile in the near-wall region of a stratified wall-bounded flow according to MOST (Monin & Obukhov, 1954) is derived by assuming the effects of stratification to be characterized by the Obukhov length-scale L defined for the case of thermally induced stratification as

$$L = \frac{u_\tau^3}{\kappa g \alpha_V q_w} \quad \text{with} \quad u_\tau^2 = \nu \left| \frac{\partial u}{\partial y} \right|_{\text{wall}}, \; q_w = k \left| \frac{\partial T}{\partial y} \right|_{\text{wall}}, \tag{1}$$

with u_τ known as the friction velocity, Kármán constant κ (Von Kármán, 1931), gravity g, thermal expansion coefficient α_V, heat flux at wall q_w, viscosity ν, mean streamwise velocity u, vertical coordinate y, thermal diffusivity k and mean temperature profile $T(y)$. The general velocity profile for the flow is then fully determined by y, the external length-scale h, u_τ, ν and L as

$$u = u_\tau F(y, h, u_\tau, \nu, L). \tag{2}$$

To simplify, the dependency on h may be dropped by limiting ourselves to the inner region classically characterized by $y/h < 1$, which we consider to be dominated by effects of viscosity and stratification only (Wyngaard, 2010). Furthermore applying the Buckingham-Π theorem (Buckingham, 1914), introducing viscous units as $u^+ = u/u_\tau$ and $y^+ = yu_\tau/\nu$ and considering $\partial_y^+ u^+$ instead of u^+ directly, we obtain

$$\frac{\partial u^+}{\partial y^+} = \frac{1}{y^+} f\left(y^+, \frac{y^+}{L^+}\right), \tag{3}$$

using $f := y^+ \partial_{y^+} F$ and viscous units for all variables as y/L=y^+/L^+ with $L^+ = Lu_\tau/\nu$. Classically, the dependency of f on two variables is addressed by limiting ourselves to the overlap region between inner- and outer flow, with the latter having y/h instead of y^+ as the characterizing coordinate and being generally defined by $y^+ > 50$. Therefore, the limit of $y^+ \to \infty$ in the inner region should yield a function independent of both y^+ and y/h, leaving y^+/L^+ as the only argument (Monin & Obukhov, 1954). Further imposing the case of moderate stratification $y^+/L^+ \lesssim 1$ then leads to the equation

$$\frac{\partial u^+}{\partial y^+} = \frac{1}{\kappa y^+}\left(1 + \beta \frac{y^+}{L^+}\right). \tag{4}$$

Integrating, one obtains the expression for the mean velocity profile in the overlap layer as given by MOST (Monin & Obukhov, 1954)

$$u^+ = \frac{1}{\kappa} \log y^+ + \frac{\beta}{\kappa} \frac{y^+}{L^+} + C(L^+), \tag{5}$$

where the integration constant can in principle depend on L^+, but is classically considered constant.
As a modification to this procedure, we propose an alternate approach by incorporating an argument employed by Jiménez & Moser (2007) for unstratified cases, according to which the variable $1/y^+$ is considered instead of y^+. An expansion including higher order terms beyond the classical zeroth-order constant $1/\kappa$ is then performed around $1/y^+ \approx 0$, i.e. $y^+ \to \infty$. We extend this argument to the stratified case by considering an expansion in both arguments at $1/y^+ \approx 0$ and $y^+/L^+ \approx 0$ simultaneously. Here, we choose to take into account terms up to second order including the cross-term of both arguments to capture effects of stronger stratification. Approximating $f \approx f_0 + f_1 + f_2$, the corresponding zeroth-, first- and second-order terms are written as

$$f_0 = \frac{1}{\kappa}, \tag{6}$$

$$f_1 = \frac{\alpha}{y^+} + \frac{\beta}{\kappa} \frac{y^+}{L^+}, \tag{7}$$

$$f_2 = \frac{\gamma}{L^+} + \frac{\alpha_2}{{y^+}^2} + \frac{\beta_2}{\kappa}\left(\frac{y^+}{L^+}\right)^2. \tag{8}$$

Here, the zeroth-order term is fixed as $1/\kappa$ so that we retain the classical log-law in the absence of stratification and second-order terms, and the coefficient β is classically scaled with the Kármán constant. The expansion of $\partial_{y^+} u^+$ up to second order thus reads

$$\frac{\partial u^+}{\partial y^+} = \frac{1}{y^+}\left(\frac{1}{\kappa} + \frac{\alpha}{y^+} + \frac{\beta}{\kappa}\frac{y^+}{L^+} + \frac{\gamma}{L^+} + \frac{\alpha_2}{{y^+}^2} + \frac{\beta_2}{\kappa}\left(\frac{y^+}{L^+}\right)^2\right). \tag{9}$$

This equation represents a second-order extension of the classical MO model with four additional terms. While such a more

complex model by itself might yield better results on a given dataset, it remains unclear whether the newly introduced terms are representative of physical processes or an improvement for the model's data-fitting capability from a purely mathematical standpoint. Therefore, we choose here to consider additional simplifications based on physical arguments to derive a set of equations with enhanced interpreteability. Firstly, both α-terms containing the reciprocal wall-distance can be discarded by assuming that their contribution will only be dominant for very small wall-distances, where the overall assumption of being close to the overlap region is not valid anymore.
Additionally, the β-terms may be addressed by limiting the model to cases where $|y^+/L^+| \ll 1$. In classical MOST this is done by considering weak stratification, i.e. $1/|L^+| \ll 1$ and y^+ limited to the overlap region, allowing to drop the second-order β_2-term (Monin & Obukhov, 1954). Alternatively, we can impose a stronger constraint on the validity region of the model with $y^+ \ll |L^+|$ without constraining the degree of stratification, similarly allowing to drop the β_2-contribution. In this case we can additionally argue to drop the linear β_1-term as well, since the linear contribution is expected to have a lesser impact on the prediction at small enough wall distances compared to the logarithmic contributions that emerge from the remaining terms. An evaluation of the first, weakly stratified approach reveals only a negligible improvement over the classical MO model and is therefore not considered further. Considering these results and the major advantage of being able to address strong stratification, we focus on the second option in the following. The corresponding, simplified equation reads

$$\frac{\partial u^+}{\partial y^+} = \frac{1}{y^+}\left(\frac{1}{\kappa} + \frac{\gamma}{L^+}\right), \tag{10}$$

where integration leads to the equation for the mean velocity profile as

$$u^+ = \underbrace{\left(\frac{1}{\kappa} + \frac{\gamma}{L^+}\right)}_{1/\kappa_{\mathrm{eff}}} \log y^+ + C(L^+). \tag{11}$$

The derived model describes a log-law with an additional stratification-dependent term in the logarithmic contribution, resulting in an effective Kármán constant given by

$$\kappa_{\mathrm{eff}} = \left(\frac{1}{\kappa} + \frac{\gamma}{L^+}\right)^{-1}. \tag{12}$$

While classical MOST neglects additional possible dependencies of the integration constant as $C(L^+)$, we choose to retain it here for generality and resolve it in alignment with the changes to the logarithmic term by using a first order expansion in $1/L^+$ as

$$C(L^+) = C_{\mathrm{eff}} = \frac{C_1}{L^+} + C, \tag{13}$$

with the final model equation reading

$$u^+ = \left(\frac{1}{\kappa} + \frac{\gamma}{L^+}\right) \log y^+ + \frac{C_1}{L^+} + C. \tag{14}$$

As expected given the underlying assumptions, the model shows a close resemblance to that of Jiménez & Moser (2007), but ultimately differs by employing the stratification measure L^+ instead of the turbulent Reynolds number Re_τ.

Analogously to the derivation presented above, a model for the temperature profile can be constructed by following the argumentation of Monin & Obukhov (1954), resulting in the additional model equation

$$T^+ = \left(\frac{1}{\kappa^{(T)}} + \frac{\gamma^{(T)}}{L^+}\right) \log T^+ + \frac{C_1^{(T)}}{L^+} + C^{(T)}, \tag{15}$$

with temperature in viscous units $T^+ = Tu_\tau/q_w$, a separate set of coefficients denoted by $^{(T)}$ and the Kármán constant for temperature $\kappa^{(T)} = 0.48$ (Von Kármán, 1931).

Both models can be interpreted as an effective extension to the classical log-law with added first order dependencies on stratification for both the logarithmic term and the integration constant and thus an effective, stratification dependent Kármán constant as defined in (12). These results are in agreement with the findings of Cheng *et al.* (2023), who also propose the existence of an effective Kármán constant based on empirical observations from DNS of the atmospheric boundary layer and atmospheric measurements. However, unlike our approach, they did not derive an analytical expression for the effective constant and instead determined its value empirically.

MODEL EVALUATION USING DNS-DATA

To evaluate the derived extended log-law for the streamwise mean velocity and temperature from equations (14) and (15), data from DNS of a thermally stratified Couette flow is used. Focusing on the fundamental effects of stratification on such a shear flow, a series of fully turbulent simulations with fixed turbulent Reynolds and Prandtl numbers and varying degrees of stable stratification are used as a basis for the analysis.
The DNS code has been employed in different works for varying boundary conditions, (Hoyas & Jiménez, 2006*a*, 2008; Avsarkisov *et al.*, 2014*a*,*b*; Kraheberger *et al.*, 2018; Lluesma-Rodríguez *et al.*, 2018). The governing equations of the system are the Navier Stokes equations under the Boussinesq approximation. These are transformed into an equation for the wall-normal vorticity ω_y and for the Laplacian of the wall-normal velocity $\phi = \nabla^2 v$. The spatial discretization uses dealiased Fourier expansions in x and z, and seven-point compact finite differences in y with fourth-order consistency and extended spectral-like resolution (Lele, 1992). The temporal discretization is a third-order semi-implicit Runge-Kutta scheme (Spalart *et al.*, 1991). Finally, the domain chosen is $(8\pi h, 2h, 3\pi h)$. The mesh has a size of $(1536, 251, 1152)$ points which gives a resolution of 8.2 and 4.1 wall units in x and z in physical space. The wall-normal grid spacing is adjusted to keep the resolution at $\Delta y = 1.5\eta$, i.e. approximately constant in terms of the local isotropic Kolmogorov scale η. Four different cases with increasing degrees of stratification are considered here with their key properties listed in table 1. A comprehensive analysis of these DNS results, including low-order statistics and turbulent budget analysis, is currently in preparation in a separate manuscript (Avsarkisov *et al.*, 2025).

Table 1. Key properties of the presented DNS simulations with a fixed Prandtl number of $Pr = 0.7$ for all cases.

Case	Re	Re_τ	Ri	Ri_τ	h/L	L^+
Ri_0	25500	1047	0.00	0	0.00	∞
Ri_{100}	43500	992	0.06	96	0.97	1023
Ri_{500}	74000	1011	0.11	472	2.65	381
Ri_{1000}	95000	988	0.13	953	3.91	252

The bulk Reynolds number Re, bulk Richardson number Ri and Prandtl number Pr are defined as

$$Re = \frac{U_w h}{\nu}, \quad Ri = \frac{g\alpha_V T_w h}{U_w^2}, \quad Pr = \frac{\nu}{k}, \tag{16}$$

with channel height $2h$, reference velocity of the walls moving in opposing directions at U_w and externally imposed wall temperatures of $\pm T_w$ at the top and bottom wall via Dirichlet boundary conditions. The corresponding friction Reynolds number Re_τ and friction Richardson number Ri_τ are given as

$$Re_\tau = \frac{u_\tau h}{\nu}, \quad Ri_\tau = \frac{g\alpha_V T_w h}{u_\tau^2}. \tag{17}$$

Notably, all cases in table 1 remain outside of the critical range of stratification-strengths at which intermittent dynamics can arise and fundamentally change the mean velocity profile, reported as $Ri > 0.15$ by Ansorge & Mellado (2014) or $L^+ < 200$ by Deusebio *et al.* (2015). The Prandtl number is kept fixed at $Pr = 0.7$ in reference to conditions from the atmospheric boundary layer. Using these DNS simulations as the empirical basis, we evaluate the derived extended log-laws from equations (14) and (15) quantitatively. Notably, a direct comparison between the extended log-law and classical MOST is deemed not productive and thus not considered in this section since the two models target different regions of the flow with the early overlap region ($10 \lesssim y^+ \lesssim 100$) and overlap/core region ($100 \lesssim y^+ \lesssim 1000$) respectively.

Mean Velocity Profiles

Velocity profiles for the DNS data and the extended log-law are displayed in Figure 1. The optimization interval for the model coefficients is chosen as $20 \leqslant y^+ \leqslant 100$ in accordance with the assumption of $y^+ \ll |L^+|$ made during the model derivation and the range $L^+ \geq 252$ contained in our datasets. A single set of coefficients is determined for all four cases since the fitted functions are considered universal for fully turbulent flows according to the theoretical derivation (Monin & Obukhov, 1954; Foken, 2006). Additional testing when determining the constants for each case individually reveals nearly identical values, confirming this theoretical assumption. The found coefficients are $\gamma = 994, C_1 = -2820$ and $C = 4.82$, as well as $\gamma^{(T)} = 1009, C_1^{(T)} = -2919$ and $C^{(T)} = 3.51$. where the large values of γ and C_1 arise correspondingly to the typical order of magnitude of L^+ for cases of significant stratification. The effective Kármán and integration constants for velocity and temperature according to equation (12) and (13) for each of the four cases are shown in table 2, indicating a steeper profile for stronger stratifications as scaled by κ_{eff}^{-1}. Most notably, we find that the observed decrease of the effective Kármán constant with stratification for velocities is in near perfect agreement with the trend reported by Cheng *et al.* (2023). Specifically, they determine a power-law of the form $\kappa_{\text{eff}}/\kappa \sim (h/L)^a$ with an exponent of $a = -0.4$ for their conducted field observations, whereas performing the same fit for our results from table 2 yields a nearly identical value of $a = -0.41$. Our analysis thus provides further evidence for a reduced effective Kármán constant in the early overlap layer following a clearly defined trend.

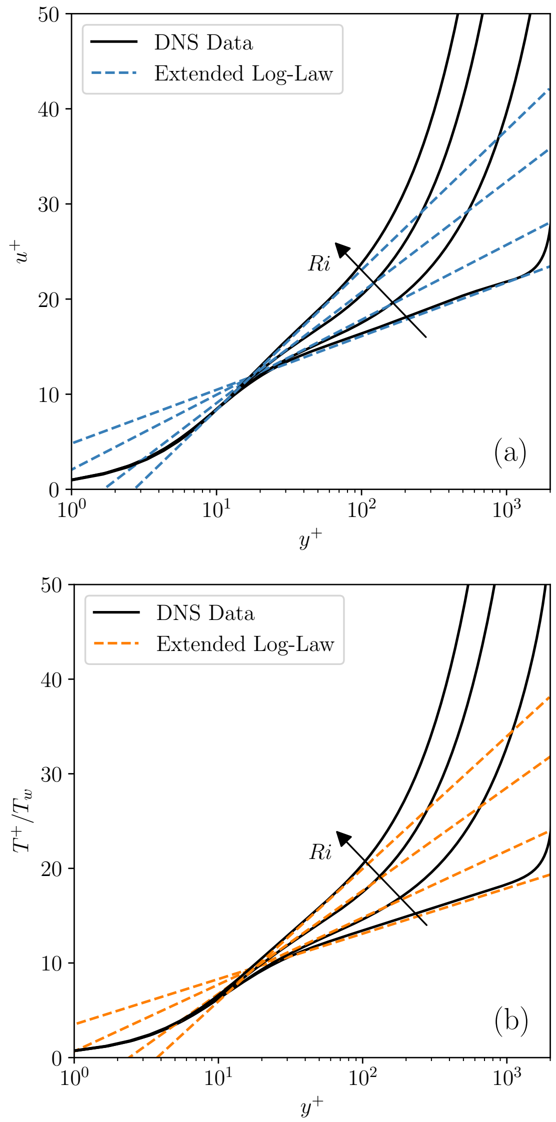

Figure 1. Vertical profiles of (a) mean streamwise velocity and (b) temperature for DNS data and the extended log-law according to equations (14) and (15) respectively.

Examining the resulting curves in Figure 1, it is apparent that results for velocity and temperature are near identical except for the axis-scaling. The extended log-law captures the data very accurately for both quantities in the beginning of the overlap layer and even beyond that down to the late buffer layer $y^+ < 50$. While this region of the boundary layer can generally not be considered universal, the result found here could be indicative of a transition at strong stratifications around $L^+ < 200$ and an associated fundamental change in the velocity profiles in this region, which allows the extended

Table 2. Effective Kármán and integration constants according to (12) and (13) for the extended log-law in (14) and (15)

Case	κ_{eff}	$\kappa_{\text{eff}}^{(T)}$	C_{eff}	$C_{\text{eff}}^{(T)}$
Ri_0	0.41	0.48	4.82	3.51
Ri_{100}	0.29	0.33	2.06	0.65
Ri_{500}	0.20	0.21	-2.58	-4.15
Ri_{1000}	0.16	0.16	-6.35	-8.06

log-law model to capture their shape at much smaller wall-distances than expected. Crucially, the estimated threshold for L^+ matches the value for which Deusebio *et al.* (2015) report the emergence of global intermittency in stratified Couette flows, thus potentially relating the found behavior to an onset of intermittent dynamics.

As a last comment, we notice that $\gamma \approx \gamma^{(T)}$, despite $\kappa \neq \kappa^{(T)}$, which seems to indicate that the influence of stratification on the logarithmic term can be described universally across velocity and temperature and potentially other quantities. This finding could thus be representative of a fundamental change in flow structure induced by stratification in the early overlap region, which would correspondingly affect multiple flow quantities similarly, as is seen for our model and in line with the findings on compensated gradients presented above.
Moreover, both values of γ are remarkably similar to the friction Reynolds numbers fixed at $Re_\tau \approx 1000$ for all four simulations used to derive the results. This could be of particular interest for further analysis, since previously not considered connections between physical quantities and model parameters could provide further physical insight into the underlying processes. Nevertheless, fully formulating and confirming such a hypothesis is not possible from the available simulations with fixed Re_τ and is therefore left for future work.

Compensated Gradients

To further investigate the observations from the previous section, the compensated gradients $y^+\partial_{y^+}u^+$ can be used to reveal additional information about the structure of the flow.
The curves for the compensated gradients are shown in Figure 2, which confirm that the extended log-law reproduces the data with good accuracy for $10 \lesssim y^+ \lesssim 100$ for both velocity and temperature. In alignment with the results from the previous section, a wide plateau emerges under increasing stratification in this region. This could be an additional indicator for the previously mentioned transition towards strong stratification around $L^+ < 200$ (Deusebio *et al.*, 2015), allowing this particular model structure to produce accurate predictions up to small wall-distances in the buffer layer. Analysis of the compensated gradients for the analogue temperature model is not explicitly shown here for brevity, but leads to qualitatively identical results.

One caveat of the presented analysis is that it is not possible to conclude from the available cases whether the plateauing of compensated gradients is indeed a limiting case that remains intact under further increasing stratification, which may be addressed in future research with a more extensive set of simulations.

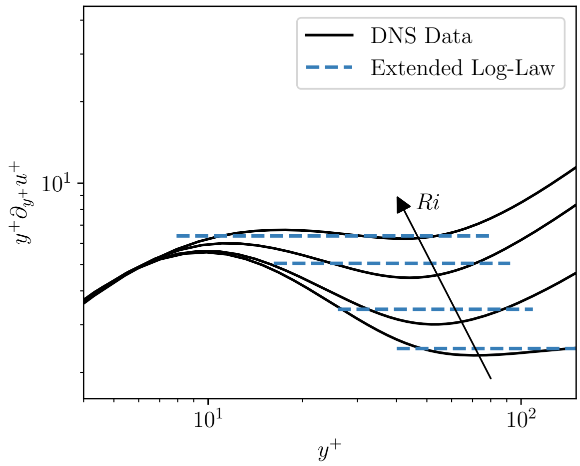

Figure 2. Compensated gradient of DNS data and the extended log-law for streamwise velocities.

CONCLUSION

In summary, this work proposes a new modeling for mean streamwise velocity and temperature profiles in the stably stratified early overlap layer with equations (14) and (15). The derivation is based on a generalization of classical Monin-Obukhov similarity theory (Monin & Obukhov, 1954) that does not assume weak stratification and extends the approach of Jiménez & Moser (2007) of employing an expansion in $1/y^+$ beyond first order to the stratified case. The resulting model focuses on the early overlap region and resembles the classical log-law with an effective, stratification-dependent Kármán constant in agreement with the trends observed by Cheng *et al.* (2023) for DNS and atmospheric measurements.
Using a set of DNS of a stratified Couette flow with smooth walls for validation, it is shown that the extended log-law is suitable to model both velocity and temperature profiles and compensated gradients accurately in the early overlap layer across a wide range of stratifications. Moreover, the model exhibits a unique capability to capture an apparent transition towards strong stratification inaccessible to classical MOST at $L^+ \sim 200$, which matches the threshold reported by Deusebio *et al.* (2015) beyond which the onset of global intermittency is observed in a stratified Couette flow.

Ultimately, the emergence of our model for strong stratification for a confined region in the early overlap layer could suggest a fundamental change in the layer-based organization of near-wall turbulence under increasing stratification. Namely, the viscous wall region and core region remain well-described by classical turbulence theory and MOST, whereas increasing stratification leads to the emergence of a third layer in between the two in the early overlap region. This newly found layer appears to be driven by a combination of both near-wall turbulence from the viscous wall region and stratified, shear-driven turbulence in the core region and is well captured by our derived log-law. Moreover the found model structure could suggest that a variable, effective Kármán constant may be a promising alternative to describe the effects of strong stratification. Examining how these key findings apply to other flow regions and scenarios to gain a better understanding of stratified turbulence as a whole may be a valuable research question to be addressed in future works.

REFERENCES

Ansorge, C. & Mellado, J. P. 2014 Global intermittency and collapsing turbulence in the stratified planetary boundary layer. *Boundary-layer meteorology* **153** (1), 89–116.

Ansorge, C. & Mellado, J. P. 2016 Analyses of external and global intermittency in the logarithmic layer of ekman flow. *J. Fluid Mech.* **805**, 611–635.

Avsarkisov, V., Hoyas, S. & Gandía-Barberá, S. 2025 DNS of the stratified plane Couette flow up to $Re_\tau, Ri_\tau = 1000$. *(In preparation)* .

Avsarkisov, V., Hoyas, S., Oberlack, M. & García-Galache, J.P. 2014*a* Turbulent plane Couette flow at moderately high Reynolds number. *J. Fluid Mech.* **751** (R1).

Avsarkisov, V., Oberlack, M. & Hoyas, S. 2014*b* New scaling laws for turbulent Poiseuille flow with wall transpiration. *J. Fluid Mech.* **746**, 99–122.

Barenblatt, G. I. & Chorin, A. J. 1997 Scaling laws and vanishing-viscosity limits for wall-bounded shear flows and for local structure in developed turbulence. *Com. on Pure and Appl. Math.* **50**, 381–398.

Barenblatt, G. I. & Monin, A. S. 1979 Similarity laws for turbulent stratified shear flows. *Archive for Rational Mechanics and Analysis* **70** (4), 307–317.

Buckingham, E. 1914 On physically similar systems; illustrations of the use of dimensional equations. *Physical review* **4** (4), 345.

Businger, J. A., Wyngaard, J. C., Izumi, Y. & Bradley, E. F. 1971 Flux-profile relationships in the atmospheric surface layer. *Journal of Atmospheric Sciences* **28** (2), 181 – 189.

Cheng, Y., Grachev, A. & van Heerwaarden, C. 2023 Logarithmic profiles of velocity in stably stratified atmospheric boundary layers. *Phys. Rev. Fluids* **8**, 114602.

Deusebio, E., Caulfield, C. P. & Taylor, J. R. 2015 The intermittency boundary in stratified plane couette flow. *J. Fluid Mech.* **781**, 298–329.

Fodor, K., Mellado, J. P. & Wilczek, M. 2019 On the role of large-scale updrafts and downdrafts in deviations from monin–obukhov similarity theory in free convection. *Boundary-layer meteorology* **172** (3), 371–396.

Foken, T. 2006 50 years of the monin–obukhov similarity theory. *Boundary-Layer Meteorology* **119**, 431–447.

Gandía-Barberá, S., Alcántara-Ávila, F., Hoyas, S. & Avsarkisov, V. 2021 Stratification effect on extreme-scale rolls in plane couette flows. *Phys. Rev. Fluids* **6**, 034605.

Grachev, Andrey, Fairall, Chris, Persson, Ola, Andreas, Edgar & Guest, Peter 2005 Stable boundary-layer scaling regimes: The sheba data. *Boundary-Layer Meteorology* **116**, 201–235.

Hoyas, S. & Jiménez, J. 2006*a* Scaling of the velocity fluctuations in turbulent channels up to $re_\tau = 2003$. *Phys. Fluids* **18** (1), 011702.

Hoyas, Sergio & Jiménez, Javier 2006*b* Scaling of the velocity fluctuations in turbulent channels up to reτ= 2003. *Physics of fluids* **18** (1).

Hoyas, S. & Jiménez, J. 2008 Reynolds number effects on the Reynolds-stress budgets in turbulent channels. *Phys. Fluids* **20** (10), 101511.

Hoyas, Sergio, Oberlack, Martin, Alcántara-Ávila, Francisco, Kraheberger, Stefanie V & Laux, Jonathan 2022 Wall turbulence at high friction Reynolds numbers. *Physical Review Fluids* **7** (1), 014602.

Jiménez, J. & Moser, R. D. 2007 What are we learning from simulating wall turbulence? *Philos. Trans. R. Soc. London, Ser. A* **365** (1852), 715–732.

Kraheberger, S., Hoyas, S. & Oberlack, M. 2018 Dns of a turbulent couette flow at constant wall transpiration up to $Re_\tau = 1000$. *J. Fluid Mech.* **835**, 421–443.

Lele, S. K. 1992 Compact finite difference schemes with spectral-like resolution. *J. Comp. Phys.* **103** (1), 16–42.

Lluesma-Rodríguez, F., Hoyas, S. & Peréz-Quiles, M.J. 2018 Influence of the computational domain on DNS of turbulent heat transfer up to $Re_\tau = 2000$ for $Pr = 0.71$. *Int. J. Heat and Mass Transfer* **122**, 983–992.

Mahrt, Larry 1998 Stratified atmospheric boundary layers and breakdown of models. *Theoretical and Computational Fluid Dynamics* **11**, 263–279.

Mater, B. D. & Venayagamoorthy, S. K. 2014 A unifying framework for parameterizing stably stratified shear-flow turbulence. *Physics of Fluids* **26** (3).

Mckeon, B. J., Li, J., Jiang, W., Morrison, J. F. & Smits, A. J. 2004 Further observations on the mean velocity distribution in fully developed pipe flow. *J. Fluid Mech.* **501**, 135–147.

Monin, A. S. & Obukhov, A. M. 1954 Basic laws of turbulent mixing in the surface layer of the atmosphere. *Contrib. Geophys. Inst. Acad. Sci. USSR* **151** (163), e187.

Monkewitz, Peter A. & Nagib, Hassan M. 2023 The hunt for the Kármán ”constant” revisited. *J. Fluid Mech.* **967**, A15.

Schlichting, Hermann & Gersten, Klaus 2016 *Boundary-layer theory*. springer.

Spalart, P. R., Moser, R. D. & Rogers, M. M. 1991 Spectral methods for the navier-stokes equations with one infinite and two periodic directions. *J. Comp. Phys.* **96** (2), 297–324.

Stiperski, I. & Calaf, M. 2023 Generalizing Monin–Obukhov similarity theory (1954) for complex atmospheric turbulence. *Phys. Rev. Lett.* **130**, 124001–1–7.

Tennekes, H. & Lumley, J. L. 1972 *A First Course in Turbulence*. *Mit Press* 1. M.I.T.Pr.

Tong, C. & Ding, M. 2020 Velocity-defect laws, log law and logarithmic friction law in the convective atmospheric boundary layer. *J. Fluid Mech.* **883**, A36.

Von Kármán, T. 1931 Mechanical similitude and turbulence. *Tech. Rep.* 611. Nat. Adv. Comm. for Aeronautics.

Wyngaard, J. C. 2010 *Turbulence in the Atmosphere*. Cambridge university press.

Yano, J.-I. & Waclawczyk, M. 2022 Nondimensionalization of the atmospheric boundary-layer system: Obukhov length and Monin–Obukhov similarity theory. *Boundary-Layer Meteorology* **182** (3), 417–439.

Zagarola, M. V. & Smits, A. J. 1998 Mean-flow scaling of turbulent pipe flow. *J. Fluid Mech.* **373**, 33–79.